Gaseous Oxygen Cooling of the Space Transportation System Launch Pad Environment

R. A. Ahmad,* E. C. Mathias,† and S. Boraas‡
Thiokol Corporation, Brigham City, Utah 84302

The external tank (ET) of the Space Transportation System (STS) contains liquid oxygen and hydrogen as oxidizer and fuel for the Space Shuttle main engines (SSMEs). During and subsequent to the loading of the ET prior to the launch of an STS, the cryogens boil in the near atmospheric conditions existing within their respective tanks. The gaseous oxygen (GOX) formed as a result of this boiling is vented overboard, mixes with air, and may, under certain wind conditions, be transported toward the STS to cause a cooling of its environment. This paper describes a two-dimensional computational fluid dynamics analysis to determine the magnitude of this cooling effect by determining the temperature depression and stratification caused by this GOX/air mixture in the region around the east redesigned solid rocket motor (RSRM), the ET, and below the STS assembly. For a severe wintertime launch temperature of 24°F (−4.44°C), the maximum local temperature depression of the mixture was calculated to be 58°F (32.22°C) in the inboard region next to the ET surface, and a surface temperature on the east RSRM was found to be as much as 25°F (13.89°C) colder than ambient. The computed average surface temperatures on either side of the RSRM were in excellent agreement with a temperature determined from a correlation of prelaunch temperature measurements.

Nomenclature

C	= concentration or mass fraction of gaseous oxygen in air
C_p	= specific heat at constant pressure; J/kg (°C), Btu/lbm (°F)
D_{12}	= binary diffusion coefficient between air and oxygen, cm^2/s
Gr	= local Grashof number, $g\beta(T_s - T_\infty)z^3/\nu^2$
g	= gravitational constant; m/s^2, ft/s^2
H_m	= mixture specific enthalpy; J/kg, Btu/lbm
h	= heat transfer coefficient; W/m^2 (°C), Btu/h-ft^2 (°F)
IX,IY,IZ	= cell numbers in domain
k	= thermal conductivity; W/m (°C), Btu/h-ft (°F)
L	= length of surface 1, 2, or 3; m, ft
(L)	= location $z = L$
M	= molecular weight; kg/kgmole, lbm/lbmole
Nu	= local Nusselt number, hz/k
P	= pressure; N/m^2, atm
Pr	= Prandtl number, $\mu C_p/k$
Ra	= Rayleigh number, $Gr\ Pr$
Sc	= Schmidt number, $\mu/\rho D_{12}$
T	= temperature; °C, °F
t	= thickness of a wall layer; m, ft
U_∞	= freestream wind velocity; m/s, ft/s
x,y,z	= Cartesian coordinates
Y	= mole fraction
(z)	= location z
β	= expansion coefficient; 1/K, 1/°R
δ	= velocity boundary layer thickness; ft, m
μ	= dynamic viscosity; $N\text{-}s/m^2$, lbm/ft-s
ν	= kinematic viscosity, μ/ρ; m^2/s, ft^2/s
ρ	= density; kg/m^3, lbm/ft^3

Subscripts

c	= critical
i	= inner, index, ith component
j	= index, jth layer
m	= mixture, measured
p	= predicted
s	= surface
t	= turbulent
1,2	= oxygen and air, respectively
∞	= freestream conditions

Superscripts

$\bar{}$	= average
$\hat{}$	= molar

Introduction

THE external tank (ET) typically contains 146,000 gal (552.61 m^3) of liquid oxygen at −297°F (−182.78°C) and 393,000 gal (1487.51 m^3) of liquid hydrogen at −423°F (−252.78°C) as oxidizer and fuel for the Space Shuttle main engines (SSMEs). Loading of the ET takes place over an approximate 6- to 8-h period prior to launch. During and subsequent to this period, the cryogens boil in the near atmospheric conditions existing within the propellant tanks; consequently, both tanks must be vented to prevent overpressurization. For safety reasons, the gaseous hydrogen is piped away from the launch pad while the gaseous oxygen (GOX) is vented overboard through two vent arms extending outward from the top of the ET. The extremely cold GOX vapor mixes with the warmer ambient air to form a mixture (GOX/air), which is colder than the ambient and, thus, negatively buoyant relative to it. The result is an induced downward flow of the mixture. Depending on the wind speed and direction at the time, this mixture may be transported toward the Space Transportation System (STS) and cause an additional cooling of its key components [redesigned solid rocket motors (RSRMs), ET, Orbiter] above and beyond the chill effect[1] produced by the ET when both cryogen tanks are filled.

Figure 1 is a top view schematic of the STS on the launch pad showing the fixed service structure (FSS) and the GOX vent ducts on the top of the ET, which are pointed in a northwest direction (280 deg). As a result of this orientation, west-

Received Aug. 25, 1990; revision received Nov. 30, 1990; accepted for publication Dec. 3, 1990.

*Associate Scientist, Aero/Thermal Section, P.O. Box 707; currently, Engineering Analysis Department. Member AIAA.

†Senior Engineer, Aero/Thermal Section, P.O. Box 707. Member AIAA.

‡Supervisor, Aero/Thermal Section; currently retired. Senior Member AIAA.

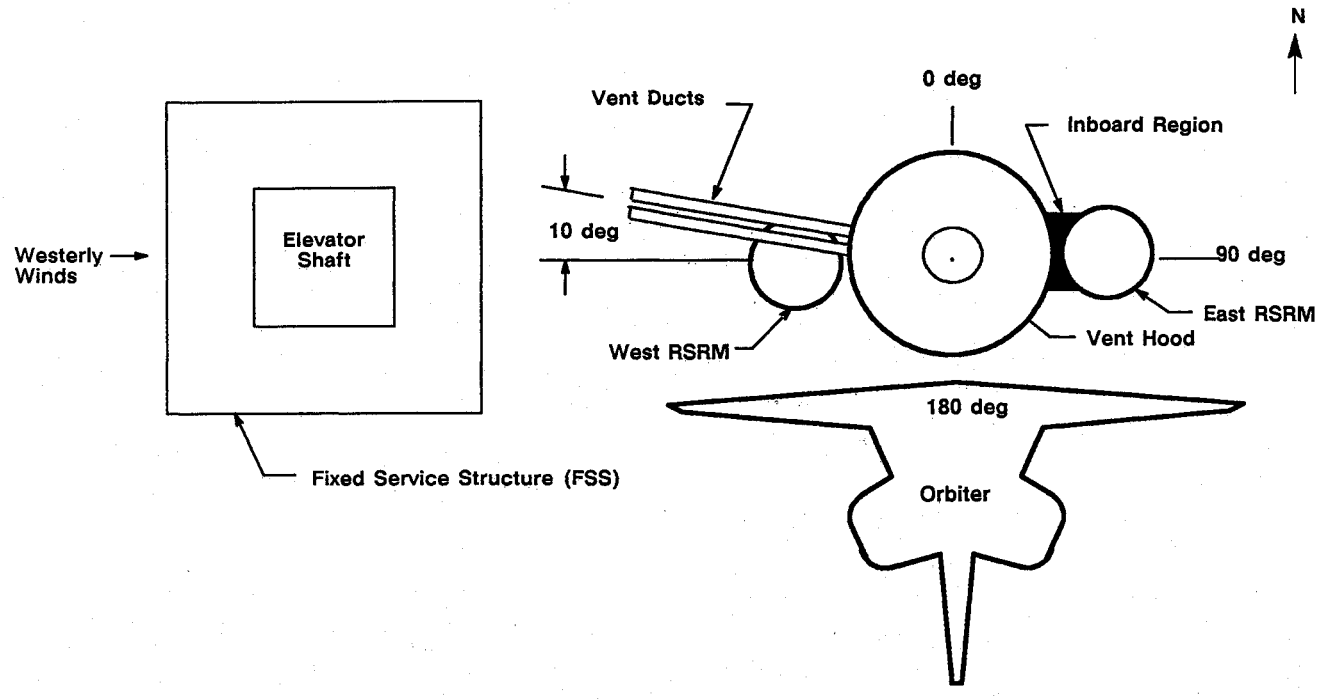

Fig. 1 Top view schematic of the STS on the launch pad.

erly winds can produce a flow on the leeward side of the FSS, which can drive the GOX vapor emerging from the ducts and the resulting mixture toward the STS. Noting that the negatively buoyant mixture already has a downward flow component, the speed and direction of the westerly wind will determine the extent to which the mixture will immerse the STS and additionally cool its components.

It was not known to what degree the GOX-cooled mixture would impose additional cooling, although an earlier one-dimensional analysis[2] suggested it could be significant. The purpose of this study was to do a more detailed two-dimensional flow/thermal calculation of the effects of the negatively buoyant flow along the length of the STS when induced by a specific concentration of GOX at the top of the STS. The analysis was done for a set of severe wintertime launch conditions, that is, for a slow westerly wind and a low ambient temperature.

The two-dimensional computational fluid dynamics (CFD) analysis was conducted using the PHOENICS '81 flow/thermal code,[3] which is a multidimensional, general purpose computer program for the analysis of fluid flow, heat transfer, and chemical reaction problems. Since only west winds can effectively carry the GOX-cooled mixture toward the assembly, the solution domain was chosen to be a westerly oriented two-dimensional slice containing the ET and the RSRM longitudinal axes. Centered relative to the 90/270-deg plane of Fig. 1, it contained sections of the ET and the RSRM and the region above these components where a mixture with a specified GOX concentration was assumed to exist as a result of a west wind. Calculations in this domain provided information on the mixture's flow/thermal properties, boundary-layer thickness, downdraft velocity, local and average surface temperatures on the ET and RSRM, GOX concentration, and local values of the temperature depression relative to the ambient.

The results of this analysis confirmed what had been suggested earlier by the one-dimensional analysis. They show that the cryogens not only play a passive role in the chilling of the RSRMs as a result of the filled ET's cold exterior surface, but also a more active part as a result of the convection of the downward flow induced by the vented GOX vapor. Future work in the determination of the effects of this induced flow is now expected to include a combined two- and three-dimensional analysis of the problem and ultimately a full three-dimensional analysis.

Discussion

This section describes the two-dimensional CFD analysis of the flow/thermal conditions within the inboard region as conducted in this study. The following subsections will discuss the governing equations, the numerical model, the boundary conditions, and the procedures for determining the thermophysical properties of the GOX/air mixture.

Governing Equations

PHOENICS '81 uses a fully conserved and implicit formulation to solve the Navier-Stokes equations and utilizes the SIMPLEST algorithm.[3] The conservation of phase mass, momentum, energy, chemical species, and other fluid properties are all expressed in PHOENICS '81 by the general partial differential equation[3]

$$\frac{\partial}{\partial t}(r_i\rho_i\phi_i) + \nabla\cdot(r_i\rho_i v_i\phi_i - r_i\Gamma_{\phi i}\,\mathrm{grad}\phi_i) = r_i S_{\phi i} \qquad (1)$$

where ϕ_i is the ith component of the conserved property ϕ, r_i and ρ_i are the volume fraction and density of ϕ_i, where $\partial/\partial t(r_i\rho_i\phi_i)$, $\nabla\cdot(r_i\rho_i v_i\phi_i)$, and $\nabla\cdot(r_i\Gamma_{\phi i}\,\mathrm{grad}\phi_i)$ denote its transience, convection, and diffusion, respectively. The term $\Gamma_{\phi i}$ is the exchange coefficient for ϕ_i, and $S_{\phi i}$ defines its source(s).

The heat conductance through the composite walls of an STS component was calculated assuming one-dimensional conduction heat transfer. Using the thicknesses t_j and thermal conductivity k_j of each jth layer of a composite wall, the conductive heat flux through n layers was calculated from

$$q''_{\mathrm{cond}} = \sum_{j=1}^{j=n}\left(\frac{k}{t}\right)_j\left[T_i - T_s(z)\right] \qquad (2)$$

where T_i is the inner surface temperature of the inner layer and $T_s(z)$ is the temperature at the outer surface. The values of the thickness and the thermal conductivity for each of the component layers in the ET and the RSRM are given in Refs. 4 and 5. In this study, the inner temperature T_i of the RSRM was the

propellant mean bulk temperature (PMBT), whereas the temperature along the entire length of the ET was conservatively chosen to be that of liquid hydrogen when, in reality, the temperature of the upper part of the ET was that of liquid oxygen. With heat conduction considered through the walls of the ET and the RSRM and heat convection at their outer surfaces, the flow/thermal analyses were truly conjugate. The conductive heat flux at a surface was treated as a heat source/sink in PHOENICS '81.

Numerical Model

In this study, the flow was assumed to be steady, two-dimensional, laminar, and elliptic. Turbulent flows are three dimensional and time dependent. Turbulence phenomena take place in eddies on the order of 1 mm in size, whereas the flow domain in this study extended over meters. Therefore, a grid fine enough to allow an accurate description of a turbulent flow would have required an immense number of cells. Thus, the choice of laminar flow was obvious.

The solution domain was a two-dimensional slice containing half of the ET and the east RSRM, their longitudinal axes, and the entrance region above them. As shown in Fig. 2, the solution domain was divided into cells with a highly nonuniform grid to permit a better resolution in areas of interest, especially within the inboard region. The two-dimensional region (77×185 ft or 23.47×56.39 m) was divided into 80 and 185 cells in the y and z directions, respectively. Twelve cells were chosen in the y direction inside the inboard region. The slice was centered on the 90/270-deg plane, as shown in Fig. 1, because the northwest orientation of the ducts was not known at the time of this study. Since the wake of the ET is so large, due to its large diameter, the coldest region along the ET would move at most by 10 deg in a clockwise direction to the $\theta = 100$ deg location (Fig. 1). However, for the severe conditions used in this study, the change in surface temperatures, due to this misalignment, would be insignificant. The thickness of the slice in the x direction was 1 ft (0.3 m). Cartesian coordinates with stepped walls were used because PHOENICS '81 has the flexibility to represent solid obstructions in the flowfield by the blockage concept.

The convergence of a solution is generally achieved by monitoring a cell within a region of the flow that is of particular interest, either from an engineering standpoint or because convergence difficulties are expected there. The PHOENICS '81 procedure for doing this and calculating continuity errors is described in Ref. 3.

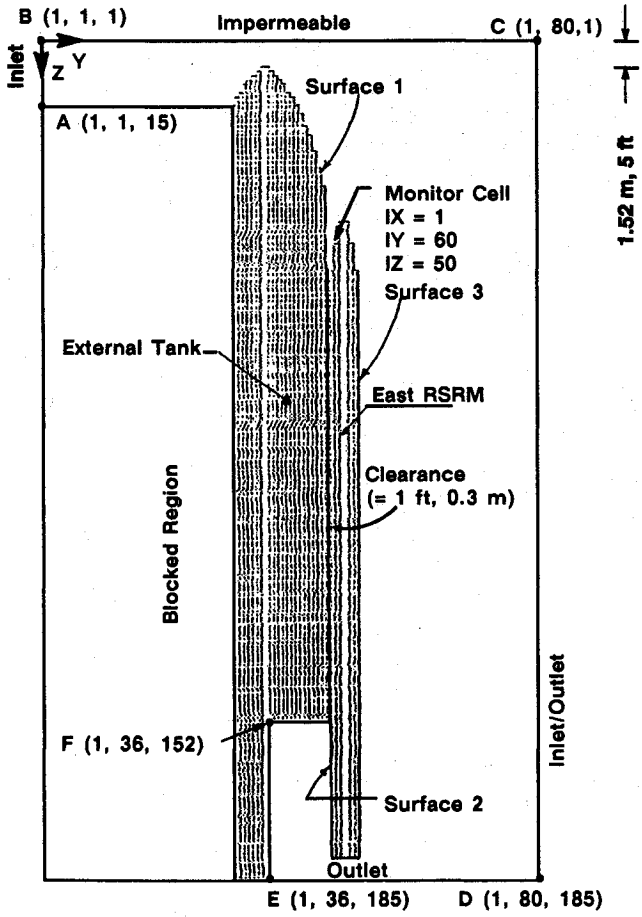

Fig. 2 Two-dimensional slice containing the ET and the east RSRM longitudinal axes (two-dimensional solution domain).

Boundary Conditions

The requirements complied with and the boundary conditions used in this study were those consistent with the most severe wintertime launch conditions experienced at Kennedy Space Center (KSC). They are as follows:

1) The ambient temperature was 24°F (−4.44°C) and the wind velocity was 1 ft/s (0.3 m/s) from the west. This was the minimum wind velocity required to transport the GOX vapor to the STS.

2) The local ambient temperature was assumed to be 15°F (−9.44°C). The reason for using this local value rather than the actual ambient was that prelaunch temperature measurements in the vicinity of the STS are usually much less than ambient. Thus a local ambient temperature of 15°F (−9.44°C) was assumed to be more appropriate in the present analysis.

3) The GOX/air mixture at the inlet (Fig. 2) of the computational domain was assumed to consist of 10% GOX vapor at −270°F (−167.78°C) and 90% air at the local ambient temperature. This 10% GOX concentration appeared to be a realistic value based on the results of the earlier one-dimensional analysis.[2] In addition to GOX concentration, velocity, mass flow rate, and enthalpy were specified as input boundary conditions along the inlet region AB.

4) Region BC of the calculation domain (Fig. 2) was assumed impermeable because it was at a height of 11 ft (3.35 m) above the vent ducts, a distance well above the expected GOX/air mixing region.

5) Regions CD and DE of the calculation domain (Fig. 2) were treated as free or constant pressure boundaries; that is, fluid was allowed to enter or exit so as to satisfy the continuity.

6) The temperature of the air in the RSRM cavity or motor bore was assumed to be 45°F (7.22°C), which was 5 deg above the lower limit on the PMBT.[6]

7) The temperature at the inner boundary of the ET for both the fuel and oxidizer tanks was conservatively assumed to be that for liquid hydrogen (−423°F or −252.78°C), as given in Ref. 7.

8) A buoyancy force term was calculated using the Boussinesq approximation, which assumes constant property conditions with the exception of a variable density; it is this variation that induces the downward fluid motion.

9) To maximize the GOX cooling effects and since most tank loadings occur during the night, solar radiation was not included. Also, thermal radiation exchange between the RSRM and the ET was not included.

10) Diffusion or convection in the third dimension (north-south direction) was neglected for two reasons. First, it permitted a maximization of the GOX cooling effect on the adjacent surfaces. Second, two dimensionality is a good assumption at the low wind speed of 1 ft/s (0.3 m/s). The 1-ft-wide region (0.3 m) can be thought of as a thick layer where relatively warm ambient air has a limited thermal penetration depth. In a three-dimensional solution of the problem, ambient conditions would be assumed far from the STS vehicle.

Thermophysical Properties of the Mixture in the Field

The mixture density ρ_m was calculated[3] as

$$\rho_m(y,z) = \rho_1(y,z)C_1(y,z) + \rho_2(y,z)C_2(y,z)$$
$$= [\rho_1(y,z) - \rho_2(y,z)]C_1(y,z) + \rho_2(y,z) \quad (3)$$

Similarly, the specific heat of the mixture $C_{p,m}$ was calculated from

$$C_{p,m}(y,z) = C_{p,1}Y_1(y,z)/M_1 + C_{p,2}[1 - Y_1(y,z)]/M_2 \quad (4)$$

The molar specific heat [Btu/lb mole (°F) or cal/g mole (°C)] for the GOX was curve fitted[8] in terms of temperature T (K) to give

$$\hat{C}_{p,1} = 7.16 + T_1/1000 - 0.4 \times 10^5(T_1)^{-2} = C_{p,1}M_1 \quad (5)$$

The specific heat of air at constant pressure was assumed constant since it only varies from 0.2405 to 0.2406 Btu/lbm (°F) [1.004 KJ/kg (°C)] between temperatures of −100°F (−73.33°C) and 100°F (37.78°C).

The thermal conductivity k_m of the mixture was calculated from the component conductivity[9] using

$$k_m(y,z) = \frac{\alpha_1(y,z)k_1(y,z) + \alpha_2(y,z)k_2(y,z)}{\alpha_1(y,z) + \alpha_2(y,z)} \quad (6)$$

where $\alpha(y,z) = Y(y,z)M^{1/3}$ and k is the component conductivity, which is approximated by Sutherland's expression[9] using the GOX and air coefficients from White[10]:

$$k_1(y,z) = 3.9417 \times 10^{-6}\left[\frac{T_m(y,z)}{491.6}\right]^{3/2}\left[\frac{491.6+400}{T_m(y,z)+400}\right] \quad (7)$$

$$k_2(y,z) = 3.8750 \times 10^{-6}\left[\frac{T_m(y,z)}{491.6}\right]^{3/2}\left[\frac{491.6+350}{T_m(y,z)+350}\right] \quad (8)$$

In these equations, T_m is the local mixture temperature in °R at every cell in the thermal field. It was calculated from the enthalpy and the specific heat of the GOX/air mixture from

$$T_m(y,z) = \frac{H_m(y,z)}{C_{p,m}(y,z)} \quad (9)$$

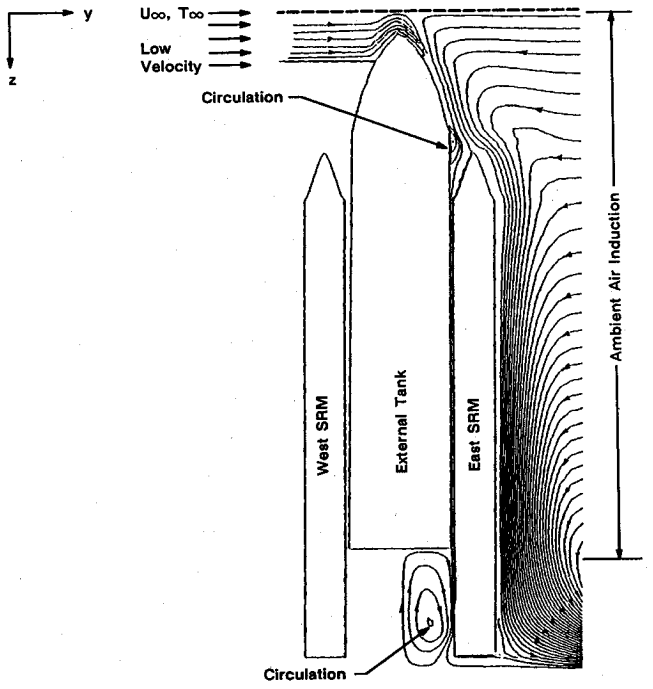

Fig. 3 Computed streamlines.

The dynamic viscosity μ_m of the low-pressure mixture was calculated from the component viscosities using the following correlation[9]:

$$\mu_m(y,z) = \frac{\lambda_1(y,z)\mu_1(y,z) + \lambda_2(y,z)\mu_2(y,z)}{\lambda_1(y,z) + \lambda_2(y,z)} \quad (10)$$

where $\lambda_i(y,z) = Y_i(y,z)(M_i)^{1/2}$. The dynamic viscosities of the GOX and air were calculated from Ref. 10 in a manner similar to that of the component thermal conductivities. These viscosities are

$$\mu_1(y,z) = 1.2896 \times 10^{-5}\left[\frac{T_m(y,z)}{491.6}\right]^{3/2}\left[\frac{491.6+250}{T_m(y,z)+250}\right] \quad (11)$$

$$\mu_2(y,z) = 1.1532 \times 10^{-5}\left[\frac{T_m(y,z)}{491.6}\right]^{3/2}\left[\frac{491.6+199}{T_m(y,z)+199}\right] \quad (12)$$

The mole fraction Y_i of either constituent in the mixture was determined as

$$Y_i(y,z) = \frac{\gamma_i(y,z)}{\gamma_1(y,z) + \gamma_2(y,z)} \quad (13)$$

where $\gamma_i(y,z) = C_i(y,z)/M_i$ and, by definition, the Schmidt number was defined as

$$Sc(y,z) = \frac{\mu_m(y,z)}{\rho_m(y,z)D_{12}(y,z)} \quad (14)$$

Finally, an expression for the diffusion coefficient between GOX and air D_{12} was developed in Ref. 11 and given as

$$D_{12}(y,z) = (a/P)\left[\frac{T_m(y,z)}{(T_{c,1}T_{c,2})^{1/2}}\right]^b\left[\frac{(T_{c,1}T_{c,2})^{5/12}}{(1/M_1 + 1/M_2)^{1/2}}\right]$$
$$\times (P_{c,1}P_{c,2})^{1/3} \quad (15)$$

where the constants $a = 2.745 \times 10^{-4}$ and $b = 1.823$ are for nonpolar gas pairs as determined from experimental data for D_{12} in cm²/s, and where P is the system pressure in atm, which, for the present launch pad analysis, is unity. The pressures $(P_{c,1}, P_{c,2})$ and temperatures $(T_{c,1}, T_{c,2})$ are values for each component at their respective critical point. They are $P_{c,1} = 49.7$ atm, $P_{c,2} = 36.4$ atm, $T_{c,1} = 154.4$ K, and $T_{c,2} = 132.0$ K. The molecular weights (M_1, M_2) are 32.0 lbm/lbmole (32 kg/kgmole) for GOX and 28.97 lbm/lbmole (28.97 kg/kgmole) for air. The temperature T_m appearing in the equation is the mixture temperature in the thermal field unless D_{12} is relatively constant, in which case the local ambient temperature was used. A typical calculated value of D_{12} is 0.16 cm²/s.

Results

The numerical model and the imposed boundary conditions were used to calculate the flow/thermal field in the vicinity of the STS. The results of this calculation are discussed below.

Flow/Thermal Field

The flow/thermal field along the ET and the east RSRM was obtained in the previously described manner with the heat transfer process between the mixture and the vehicle surface assumed to be natural convection. The diffusion in the GOX/air mixture was appropriately accounted for at all times through the solution of the concentration equations. The results showed that the characteristics of the flow/thermal field were dependent on the velocity entering the inlet (region AB) to the calculation domain as well as the mixture density, ambient temperature, surface temperature, binary diffusion coefficient, and the STS geometry.

The GOX/air mixture, as a consequence of its negative buoyancy, is shown to descend along the length of the STS vehicle, as evidenced by the streamlines in Fig. 3. It also in-

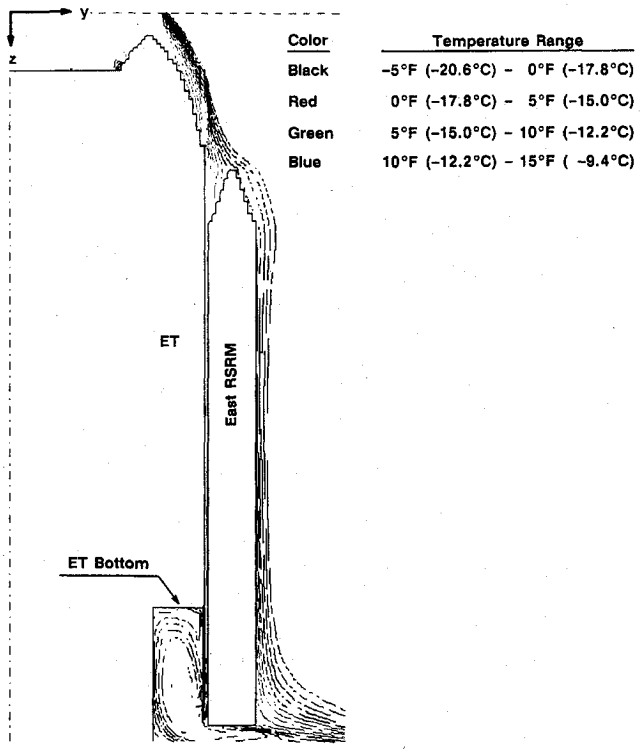

Fig. 4 Computed mixture isotherms in solution domain.

duces and entrains an ambient flow across the inlet portion of region CD, which is initially directed toward the east sides of both the ET and the east RSRM but which becomes directed downward and then away from the STS near its base and then across the outlet portion of region CD. Flow out of the inboard region results in a recirculation below the ET with an outflow under the bottom of the RSRM and across the CD outlet region.

Although the current analysis involved the solution of the Navier-Stokes equations and the energy equation, it was desirable to calculate the velocity boundary-layer thickness based on the Eckert-Jackson correlation[12,13] for turbulent free convection flow along a single vertical plate. This was done to assess the results of this study by obtaining the convective heating rates along the three surfaces of the two-dimensional domain. The calculations were made using the thermal field and the thermal properties computed in the present analysis. The velocity boundary-layer thickness along surfaces 1, 2, and 3, as identified in Fig. 2, were calculated as a function of the distance measured from the top of each surface. These were calculated[4,5] using the correlation and assuming that, in each instance, the surface in question was vertical and isolated from the other two. It was obvious from these calculations that, unhindered, the boundary layer can become very large over the distances encountered along the STS components. The inboard region starts at approximately 15 ft (4.57 m) from the top of the RSRM and approximately 50 ft (15.24 m) from the top of the ET. Therefore, at the entrance to the inboard region, δ on the ET surface is about 1.6 ft (0.49 m), whereas on the RSRM, δ is 0.8 ft (0.24 m). Since their sum exceeds the 1-ft (0.3-m) clearance, mixed flow would be expected downstream of the inboard region entrance. Thus, the characteristics of a single boundary-layer flow along a vertical plate is not realized within the inboard region. This means that the temperature and velocity profiles along either surface in the inboard region are different from those along the surface of a heated or cooled vertical plate.

The downdraft velocity on the outer surface 3 of the RSRM was calculated[4,5] from an expression for the the downdraft velocity profile as derived by Eckert-Jackson[12,13] for a turbulent free convection flow along a single, vertical surface. The downdraft velocity was shown to exceed 5 ft/s (1.52 m/s) near the surface of the RSRM but decreases as the distance normal to the surface increases. The larger velocity is due to the colder and more dense GOX/air mixture near the RSRM surface.

Figure 4 shows the isotherms of the GOX/air mixture in the solution domain. Temperatures as cold as $-34°F$ ($-36.67°C$) were calculated at the bottom of the inboard region and adjacent to the ET, and temperatures of 5 to 10°F (-15 to $-12.22°C$) were calculated next to the RSRM surface in the inboard region. The $-34°F$ ($-36.67°C$) temperature represents a temperature depression of 58°F (32.22°C). Below the ET, the maximum temperature depression was 17°F (9.44°C). The temperatures along most of the upper surface of the domain, that is, the impermeable region BC (Fig. 2), and along the inlet portion ($0 \le z \le 180$) of the CD region on the right side of the domain were ambient, as expected, based on the size selected for the domain. The temperatures were lower than ambient along the outlet portion ($180 \le z \le 185$) of the CD region due to the outflow in this region. However, this region is too far (29.5 ft or 8.99 m) from the surface of the east RSRM to have any influence on the solution.

Surface Temperatures

Computed Temperatures

The temperatures on surfaces 1, 2, and 3 were not known, a priori, and had to be calculated. This precluded using the surface temperature along with the ambient temperature as thermal drivers. Therefore, the inner temperatures of the ET and the RSRM were used as the thermal boundary conditions along with the ambient temperature. The surfaces were neither isothermal nor a part of the grid network. Consequently, at a point on a surface, the surface temperature had to be determined by an extrapolation from the mixture temperatures in the adjacent cells. This was accomplished using a Lagrange polynomial[14] of the second order:

$$T_s(y_s,z) = \sum_{j=1}^{3} T_m(y_j,z) \frac{\prod_{\substack{i=1 \\ i\neq j}}^{3} (y_s - y_i)}{\prod_{\substack{i=1 \\ i\neq j}}^{3} (y_j - y_i)} \tag{16}$$

where T_m is the mixture temperature in the cells adjacent to the surface, y_s the surface distance, and y_i and y_j are distances to the centers of the adjacent cells, as defined for each of the three surfaces (surfaces 1, 2, 3). Figures 5 show the surface temperatures, the mixture temperatures (T_1, T_2, and T_3) in the adjacent cells, and the average surface temperature along surfaces 1, 2, and 3.

The calculated surface temperature of the ET (surface 1) is shown in Fig. 5a as a function of the distance along its surface as measured from the top of the ET. Calculated using Eq. (16), it was found to vary from 3°F ($-16.11°C$) at the top to $-61°F$ ($-51.67°C$) at the bottom, the latter representing an 85°F (47.22°C) surface temperature depression. This computed temperature of $-61°F$ ($-51.67°C$) near the bottom of the ET was probably much greater than what would be the actual value. There are several possible explanations for this. First, the calculations were made for the ET surface within the inboard region, which was where the coldest surface temperatures would be expected because of the region's confining effect on the cold downward flow. Second, the two dimensionality of the analysis of the inboard region precluded the mixing of the cold downward flowing mixture with the warmer ambient. Finally, the assumptions of a local ambient temperature of 15°F ($-9.44°C$) instead of the actual 24°F ($-4.44°C$), the conservative internal boundary temperature of $-423°F$ ($-252.78°C$) for both the oxygen and hydrogen tanks, and the absence of solar heat flux in this analysis may have contributed to the calculation of this very low temperature. The average

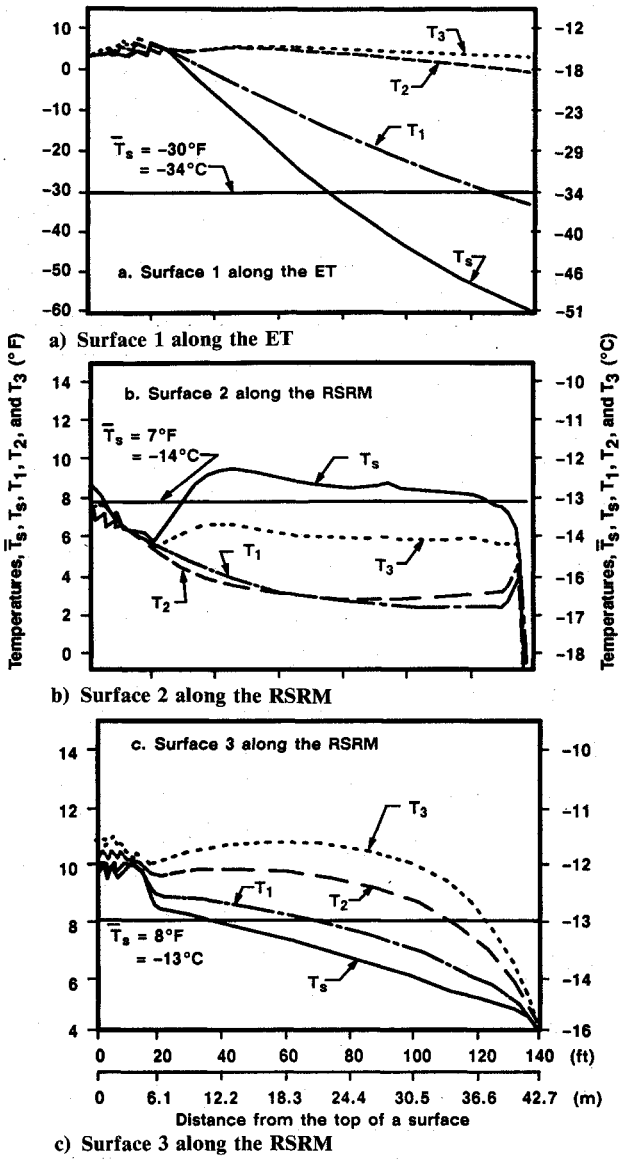

Fig. 5 Temperatures on the surface and in the adjacent cells along surfaces 1, 2, and 3 of Fig. 2.

surface temperature of the ET was calculated to be −30°F (−34.44°C) by numerically integrating the local values. From this, it is apparent that the local surface temperature is of greater importance than the average temperature when cold or hot spots are being considered.

The calculated RSRM surface temperature on surface 2, which faces the ET, is shown in Fig. 5b as a function of distance along the surface of the RSRM measured from its top. The RSRM surface temperature was found to vary from 9°F (−12.78°C) at its top to −1°F (−18.33°C) at its bottom with the average surface temperature being 7°F (−13.89°C). Therefore, the inboard surface of the RSRM was 15 to 25°F (8.33 to 13.89°C) colder than ambient. Most of this temperature drop took place on the portion of the RSRM surface which was below the ET and was thought to be due to the recirculation region that was present there (Figs. 3 and 4). At the 100-ft (30.48-m) distance, which was approximately the aft field joint location, the surface temperature was approximately 8°F (−13.33°C). This temperature compares with the 0°F (−17.78°C) temperature calculated previously for this joint using the one-dimensional analysis.[2] The 8°F (−13.33°C) temperature difference is not too surprising when one considers that the present two-dimensional analysis would be expected to give higher mixture temperatures in the inboard region as a result of the ambient air induction into the computational domain, a possibility that did not exist in the one-dimensional analysis. This induction is due to the heat sink represented by the cold surfaces. Despite this difference, and other differences between the two analyses, it is important to note that both predict a marked cooling effect of the GOX on the flow within the inboard region.

The calculated RSRM surface temperature on the east or outer side of the RSRM (surface 3) is shown in Fig. 5c, again as a function of distance from the top of the RSRM. These results show that this temperature varies from 10°F (−12.22°C) at the top to 4°F (−15.56°C) at the bottom with the average surface temperature being 8°F (−13.33°C). Thus one concludes that the cooling effect of the GOX vapor is not limited to the inboard region but has an effect on other regions within the STS launch pad environment as well.

The relatively cold subambient temperatures calculated on surfaces 1, 2, and 3 bear further testimony to the cooling effect the vented GOX vapor has on the STS environment. These results were not totally unexpected in view of the results of two earlier studies.[13,15] In the first of these studies,[15] an attempt was made to determine the cooling effect on the SRM surface facing the ET (surface 2 in this study) when this surface was intersected by a free convection boundary layer as a result of its growth along the surface of the fully loaded ET. With an assumed ambient temperature of 23°F (−5°C) in a quiescent (no wind) environment, the minimum surface temperature calculated along the RSRM was found to be near ambient (23.5°F or −4.72°C) while the minimum temperature on the ET was −29.5°F (−1.39°C) or 52.5°F (29.17°C) below the ambient. Since this earlier study did not include the effect of the GOX vapor, the larger ET surface temperature depression of 59°F (32.78°C), as calculated in this study, came as no surprise.

The second study[13] dealt with the free convective flow within what is defined as the inboard region in this study. The analysis was done for a 1-kt (0.52-m/s) west wind, an ambient temperature of 38°F (3.33°C), and an assumed ET surface (surface 1 in this study) temperature of 10°F (−12.22°C). The temperature on the SRM surface (surface 2 in this study) was calculated to be 34.5°F (1.39°C) or 3.5°F (1.94°C) colder than ambient. This 3.5°F (1.94°C) cooling of the SRM surface in the absence of the vented GOX effluent is certainly much less than the 15 to 25°F (8.33 to 13.89°C) cooling effect that was actually determined in this study for the RSRM surface when the GOX vapor is present. Thus, the surface temperatures predicted in this study are much lower than estimates from these earlier studies.

Surface Temperature Correlations

References 16 and 17 provide information on prelaunch surface temperature measurements made on the lower surfaces of the east and west SRMs and RSRMs during 27 launches of the STS. Shown in Table 1, these measured temperatures $T_{s,m}$ were correlated in this study as a function of the ambient temperature to give the following expressions for the surface temperature:

East motors:

$$T_s(°F) = 1.059\,T_\infty(°F) - 6.979 \tag{17a}$$

or

$$T_s(°C) = (5/9)\left[T_s(°F) - 32\right] \tag{17b}$$

West motors:

$$T_s(°F) = 0.898\,T_\infty(°F) + 3.632 \tag{18a}$$

or

$$T_s(°C) = (5/9)\left[T_s(°F) - 32\right] \tag{18b}$$

Table 1 Lower solid rocket motor/redesigned solid rocket motor temperature history

				East SRM			West SRM		
n	Launch	Date	T_∞, °F(°C)	$T_{s,m}$, °F(°C)	$T_{s,p}$, °F(°C)	ΔT,[a] °F(°C)	$T_{s,m}$, °F(°C)	$T_{s,p}$, °F(°C)	ΔT,[a] °F(°C)
1	51-I	08-24-85	83(28)	82(28)	85(29)	−3(−1)	82(28)	78(26)	4(2)
2	51-J	10-03-85	79(26)	79(26)	79(26)	0(0)	82(28)	74(23)	8(5)
3	STS-31	11-26-85	78(26)	86(30)	78(26)	8(4)	84(29)	73(23)	11(6)
4	STS-28	09-12-85	77(25)	84(29)	76(24)	8(5)	82(28)	73(23)	9(5)
5	STS-27	08-25-85	77(25)	77(25)	76(24)	1(1)	77(25)	73(23)	4(2)
6	——	08-27-85	75(24)	77(25)	73(23)	4(1)	77(25)	71(22)	6(3)
7	STS-24	04-29-85	73(23)	48(9)	71(22)	−23(−13)	47(8)	69(21)	−22(−13)
8	STS-25	06-16-85	72(22)	70(21)	69(21)	1(0)	72(22)	68(20)	4(2)
9	——	01-10-86	67(19)	65(18)	63(17)	2(1)	65(18)	64(18)	1(0)
10	STS-32	01-07-86	65(18)	65(18)	63(17)	2(1)	63(17)	64(18)	1(−1)
11	——	01-12-86	65(18)	59(15)	60(16)	−1(−1)	62(17)	62(17)	0(0)
12	STS-23	04-12-85	65(18)	69(21)	60(16)	9(5)	67(19)	62(17)	5(2)
14	——	12-19-85	56(13)	60(16)	50(10)	10(6)	60(16)	55(13)	5(3)
15	——	01-06-86	56(13)	61(16)	49(9)	12(7)	52(11)	54(12)	2(−1)
16	——	12-19-85	56(13)	60(16)	49(9)	12(7)	60(16)	54(12)	6(4)
16	——	01-27-86	43(6)	34(1)	34(1)	0(0)	38(3)	43(6)	−5(−3)
17	STS-33	01-28-86	28(−2)[b]	14(−10)	18(−8)	−4(−2)	28(−2)	29(−2)	−1(0)
18	STS-26	09-29-88	84(29)	74(23)	86(30)	−12(−7)	62(17)	79(26)	−17(−9)
19	STS-27	12-02-88	54(12)	56(13)	46(8)	10(5)	56(13)	52(11)	4(2)
20	STS-29	03-13-89	65(18)	56(13)	60(16)	−4(−3)	59(15)	62(17)	−3(−2)
21	STS-30	05-04-89	78(26)	72(22)	78(26)	−6(−4)	74(23)	73(23)	1(0)
22	STS-28	08-08-89	80(27)	74(23)	80(27)	−6(−4)	75(24)	75(24)	0(0)
23	STS-34	10-18-89	84(29)	77(25)	86(30)	−9(−5)	75(24)	79(26)	−4(−2)
24	STS-33	11-22-89	66(19)	59(15)	61(16)	−2(−1)	59(15)	63(17)	−4(−2)
25	STS-32	01-08-90	52(11)	53(12)	44(7)	9(5)	54(12)	51(11)	3(1)
26	STS-36	02-28-90	65(18)	64(18)	60(16)	4(2)	62(17)	62(17)	0(0)
27	STS-31	04-24-90	70(21)	66(19)	67(19)	−1(0)	64(18)	66(19)	−2(−1)

[a] $\Delta T = T_{s,m} - T_{s,p}$.
[b] Shown as 23°F (−5°C) and 24°F (−4.44°C) as in Refs. 15 and 2, respectively.

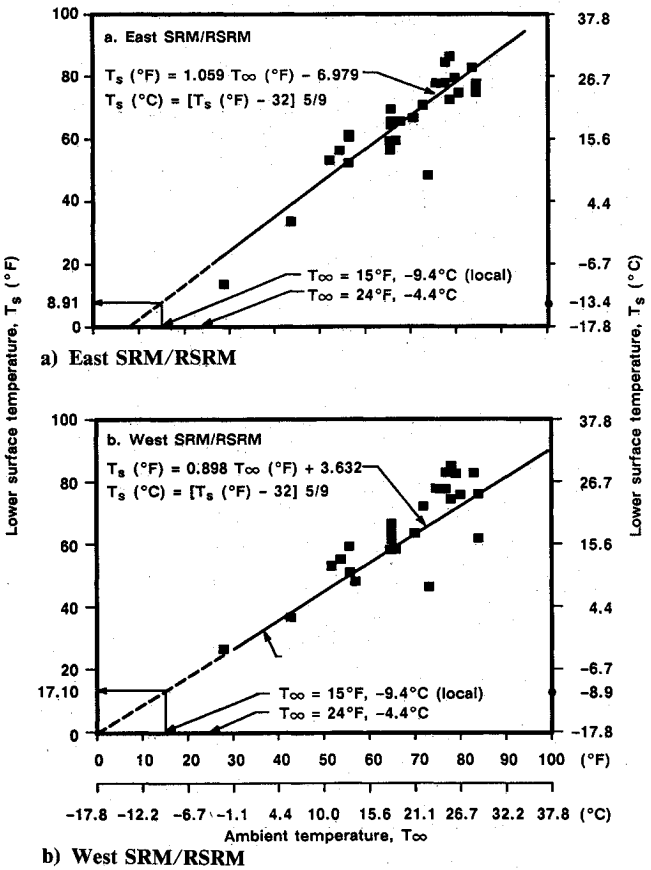

Fig. 6 East and west SRM/RSRMs lower surface temperatures as measured prior to launch.

These correlations are shown in Figs. 6. Given the scatter of the data and the limited amount at lower temperatures, extrapolation to low temperatures is still reasonable.[18] That is, the inclusion of the lowest measured temperature at an ambient temperature of 28°F (−2.22°C), as shown in Fig. 6a, is valid. Neither the wind speed nor the wind direction was included in the development of these correlations. Table 1 includes predicted surface temperature $T_{s,p}$ using these correlations as well as denoting the difference ΔT between the measured and predicted values.

Figure 6a shows that, upon extrapolating the correlation toward a 0°F (−17.78°C) ambient, the expected surface temperature on the east RSRM would be 8.91°F (−12.83°C) for the 15°F (−9.44°C) local ambient used in the present analysis. This is in excellent agreement with the average values of 7°F (−13.89°C) and 8°F (−13.33°C) that were calculated for surfaces 2 and 3, respectively. This agreement may be somewhat fortuitous since the analysis was limited to a two-dimensional assessment and the choice of a local temperature was somewhat arbitrary. However, the fact that this combination of analytical approach and local temperature concept led to this agreement adds credibility to the assumed 10% GOX concentration at the entrance to the inboard region, as indicated earlier by the results of the one-dimensional analysis.[2]

The surface temperatures on the west SRM/RSRMs were also correlated, even though these motors were not considered in the present analysis. A comparison of the correlations in Figs. 6 shows that the lower surface on the east SRM/RSRMs is colder than that on the west SRM/RSRMs. This had been anticipated at the start of this study when the decision was made to primarily model and analyze the flow, thermal, and concentration fields around the east RSRM.

Heat Transfer

Heat transfer calculations (heat transfer coefficient or the Nusselt number) were not the primary objective of this study. To validate the results of this study (coupled flow and thermal fields, calculated quantities at the surfaces such as surface temperatures and Grashof number), an attempt was made to calculate heat transfer results using a well-established correlation given by Eckert-Jackson.[12,13] This correlation applies to turbulent free convection along an isothermal, single heated/cooled vertical flat plate in air. Another reason for considering heat transfer was to validate the assumption of treating the

cylindrical components (RSRMs, ET) of the STS as vertical flat plates, using available heat transfer theory on free convection along a single vertical flat plate.

The heat transfer rate is commonly expressed in terms of the local or average heat transfer coefficient or the dimensionless Nusselt number.

The local heat transfer coefficient was calculated as

$$h(z) = Nu(z)k_m(y_s,z)/z$$
$$= 0.0295\left[\frac{Gr(z)}{Pr_t(z)}\right]^{2/5}[Pr(z)]^{7/15}\frac{k_m(y_s,z)}{z} \quad (19)$$

and is shown in Fig. 7 for surfaces 1, 2, and 3 along with the average heat transfer coefficient, which was calculated as

$$\bar{h}(L) = \overline{Nu}(L)\bar{k}_m/L$$
$$= 0.0246\left[\frac{Gr(L)}{Pr_t(L)}\right]^{2/5}[Pr(L)]^{7/15}\frac{\overline{k_m}(L)}{L} \quad (20)$$

where

$$\overline{Gr}(L) = g\beta\left[\bar{T}_s(L) - T_\infty\right]L^3/\left[\bar{\nu}(L)\right]^2 \quad (21)$$

is the average Grashof number.

For vertical plates, the critical Grashof number corresponding to transition to turbulence is $Gr(z)_c \simeq 1.43\times10^9$ and the corresponding critical Rayleigh number is $Ra(z)_c = Gr(z)_c Pr(z) \simeq 10^9$.

The Rayleigh numbers at the end of surfaces 1, 2, and 3 are larger than the critical value by factors of 1.05×10^6, 1.70×10^5, and 1.1333×10^5, respectively. Moreover, the average calculated Rayleigh number for any of the three surfaces is higher than the critical Rayleigh number. Because of the Rayleigh number's dependency on the cube of the length and the large length associated with the RSRMs and the ET, the Rayleigh numbers obtained in this study (up to 10^{15}) were three orders of magnitude larger than the largest (10^{12}) reported in the literature. Therefore, the correlations in the literature may not apply to the present problem because their range of applicability is limited to lower Rayleigh numbers. Since surface 3 is relatively warmer than surface 2, the average Rayleigh number along surface 3 is 7.4% higher than that of surface 2, even though the mixture thermal properties are the same.

Reference 19 states that a vertical cylinder may be treated as a flat vertical plate when

$$\left(\frac{D}{L}\right) \geq \frac{35}{\left[\overline{Gr}(L)\right]^{1/4}} \quad (22)$$

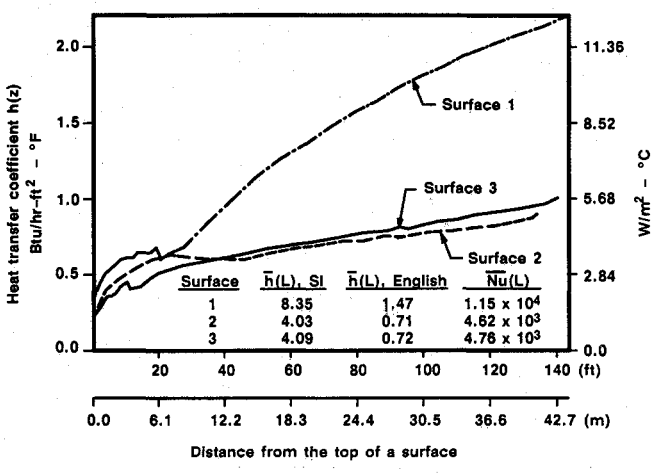

Fig. 7 Local and average heat transfer coefficients along surfaces 1, 2, and 3 of Fig. 2.

where D is the diameter of the cylinder and L is the characteristic length. Applying this equation to the ET ($D = 28$ ft or 8.54 m) and the RSRM ($D = 12$ ft or 3.66 m) where $L = 140$ ft (42.67 m) for both and then using the previously calculated average Grashof numbers of 3.09×10^{14}, 3.15×10^{13}, and 3.4×10^{13} for surfaces 1, 2, and 3, respectively, it was shown that this requirement was met. That is, the assumption of treating the cylindrical components (RSRMs, ET) of the STS as vertical flat plates is valid.

References 4 and 5 provide additional details on the present two-dimensional study. They include information on the velocity boundary-layer thickness, the downdraft velocity as a function of the length, the characteristic velocity, the relative values of the laminar and turbulent Prandtl numbers along each of the three surfaces, the thermal conductivity of the mixture adjacent to each surface, and the temperature gradient of the mixture along each surface.

The results of this study indicate that the vented GOX vapor can have a significant cooling effect on the STS launch pad environment. Since this has not been firmly established, more detailed two- and three-dimensional analyses will be conducted in the future.

Conclusions

The following statements summarize the results of the analysis and the conclusions that were reached.

1) The minimum temperature of the negatively buoyant GOX/air mixture was found to be −34°F (−36.67°C) near the base of the inboard region and adjacent to the ET. Representing a 58°F (32.22°C) temperature depression, it is comparable to the 52.5°F (29.17°C) temperature depression calculated in Ref. 15 in the absence of GOX vapor.

2) The predicted surface temperatures along the inboard surface of the ET ranged from 3°F (−16.11°C) at the top to −61°F (−51.67°C) at the bottom, where the latter, although possibly too low, emphasizes the potential severity of GOX cooling.

3) The RSRM inboard surface temperatures varied from 9°F (−12.78°C) at the top to −1°F (−18.33°C) at the bottom, giving an 8°F (−13.33°C) temperature at the aft field joint location and an average 7°F (−13.89°C) temperature along the surface.

4) The surface temperatures on the outer surface of the RSRM varied from 10°F (−12.22°C) at the top to 4°F (−15.56°C) at the bottom, giving an average temperature of 8°F (−13.33°C) along the surface.

5) The predicted 8°F (−13.33°C) temperature for the aft field joint in the inboard region of the RSRM was, as expected, somewhat warmer than the 0°F (−17.78°C) temperature predicted for this joint with the more conservative one-dimensional analysis.[2]

6) The computed average surface temperatures of 7°F (−13.89°C) and 8°F (−13.33°C) on the inboard and outer surfaces of the RSRM are in excellent agreement with the predicted temperature of 8.91°F (−12.83°C), as obtained from a correlation of the east SRM/RSRM prelaunch motor temperatures from 27 STS flights. Although this agreement may be due to the combination of a two-dimensional analysis and the choice of local ambient temperature, it does suggest that GOX vapor has an appreciable cooling effect.

7) This agreement of the surface temperatures lends credibility to the assumed 10% GOX concentration suggested by the previous one-dimensional analysis[2] and used in this study.

References

[1]Ahmad, R. A., and Boraas, S., "External Tank Chill Effect on the Space Transportation System Launch Pad Environment," *Journal of Spacecraft and Rockets*, Vol. 28, No. 3, 1991, pp. 306–314.

[2]Boraas, S., and Buttars, R. L., "Pre-Launch Temperature Prediction Model (Response to Action Item SRMTF-02-07-011)," Morton Thiokol, Inc., Brigham City, UT, TWR-15796, June 1987.

[3]Singhal, A. K., and Owens, S. F., "Introduction to PHOENICS," CHAM of North America, Feb. 1984.

[4]Ahmad, R. A., and Mathias, E. C., "Free Convection Around the Space Shuttle on the Launch Pad," Morton Thiokol, Inc., Brigham City, UT, TWR-18170, March 1988.

[5]Ahmad, R. A., Boraas, S., and Mathias, E. C., "Gaseous Oxygen Cooling of the STS Launch Pad Environment: Model Validated by STS-33 Data," Thiokol Corp., Brigham City, UT, TWR-60543, May 1990.

[6]Anon., "CEI Specification (CPW1-3600A, Paragraph 3.2.1)," Morton Thiokol, Inc., Brigham City, UT, Aug. 1987.

[7]Anon., "Space Shuttle External Tank, Thermal Data Book," Martin Marietta Corp., Michoud Div., Mississippi, June 1981.

[8]Smith, J. M., and Van Ness, H. C., *Introduction to Chemical Engineering Thermodynamics,* 3rd ed., McGraw-Hill, New York, 1975, Chap. 4.

[9]Perry, R. H., and Chilton, C. H., *Chemical Engineers' Handbook,* 5th ed., McGraw-Hill, New York, 1973, Chap. 3.

[10]White, F. M., *Viscous Fluid Flow,* McGraw-Hill, New York, 1974, Chap. 1.

[11]Bird, R. B., Stewart, W. E., and Lightfoot, E. N., *Transport Phenomena,* Wiley, New York, 1960, Chap. 16.

[12]Chapman, A. J., *Heat Transfer,* 3rd ed., Macmillan, New York, 1974, Chap. 9.

[13]Anon., "Documentation of Convective CFD Analytical Support to the TIDDB Verification," Rockwell Int., Rept. No. 112-041-B11-01, Huntsville, AL, Oct. 1987.

[14]Hornbeck, R. W., *Numerical Methods,* Prentice-Hall, Englewood Cliffs, NJ, 1975, pp. 43–45.

[15]Anon., "Thermal Modeling of the Space Shuttle Launch Configuration," SRS Technologies, SRS/STD-TR86-022, Huntsville, AL, March 1986.

[16]Katnik, G. N., Speech, R. F., and Stevenson, C. G., "STS-33 TPS, Ice/Frost, and Debris Team Report," Vols. 1 and 2, Attachment A-7, Kennedy Space Center, FL, March 1986.

[17]Anon., "Thiokol Flight Motor Set Final Report," Thiokol Corp., Repts. TWR-17540-1 through TWR-17544-10 for flights STS-26 through STS-31, Brigham City, UT, Sept. 1988 through April 1990.

[18]Meyers, R. H., *Classical and Modern Regression with Applications,* Duxbury, Boston, MA, 1986, Chap. 8.

[19]Holman, J. P., *Heat Transfer,* 4th ed., McGraw-Hill, New York, 1976, Chap. 7.

James A. Martin
Associate Editor